Since January 2020 Elsevier has created a COVID-19 resource centre with free information in English and Mandarin on the novel coronavirus COVID-19. The COVID-19 resource centre is hosted on Elsevier Connect, the company's public news and information website.

Journal of Critical Care 60 (2020) 169–176

Contents lists available at ScienceDirect

Journal of Critical Care

journal homepage: www.journals.elsevier.com/journal-of-critical-care

Quantitative-analysis of computed tomography in COVID-19 and non COVID-19 ARDS patients: A case-control study

Louis Chauvelot [a], Laurent Bitker [a,c], François Dhelft [a,c], Mehdi Mezidi [a,b], Maciej Orkisz [c], Eduardo Davila Serrano [c], Ludmilla Penarrubia [c], Hodane Yonis [a], Paul Chabert [a], Laure Folliet [a], Guillaume David [a], Judith Provoost [a], Pierre Lecam [a], Loic Boussel [c,d], Jean-Christophe Richard [a,c,*]

[a] Service de Médecine Intensive Réanimation, Hôpital De La Croix Rousse, Hospices Civils de Lyon, 93 grande rue de la Croix-Rousse, 69004 Lyon, France
[b] Université de Lyon, Université Claude Bernard Lyon 1, 43 boulevard du 11 Novembre 1918, 69622 Villeurbanne, Cedex, France
[c] Université de Lyon, Université Claude Bernard Lyon 1, INSA-Lyon, UJM-Saint Etienne, CNRS, Inserm, CREATIS UMR 5220, U1206, F-69621, 7 Avenue Jean Capelle, 69621 Villeurbanne, France
[d] Service de Radiologie, Hôpital De La Croix Rousse, Hospices Civils de Lyon, 93 grande rue de la Croix-Rousse, 69004 Lyon, France

ARTICLE INFO

Keywords:
Acute respiratory distress syndrome
Computed tomography
Transpulmonary pressure
Tidal hyperinflation
Driving pressure
COVID-19

ABSTRACT

Purpose: The aim of this study was to assess whether the computed tomography (CT) features of COVID-19 (COVID+) ARDS differ from those of non-COVID-19 (COVID−) ARDS patients.
Materials and methods: The study is a single-center prospective observational study performed on adults with ARDS onset ≤72 h and a $PaO_2/FiO_2 \leq 200$ mmHg. CT scans were acquired at PEEP set using a PEEP-FiO_2 table with VT adjusted to 6 ml/kg predicted body weight.
Results: 22 patients were included, of whom 13 presented with COVID-19 ARDS. Lung weight was significantly higher in COVID− patients, but all COVID+ patients presented supranormal lung weight values. Noninflated lung tissue was significantly higher in COVID− patients (36 ± 14% vs. 26 ± 15% of total lung weight at end-expiration, $p < 0.01$). Tidal recruitment was significantly higher in COVID− patients (20 ± 12 vs. 9 ± 11% of VT, $p < 0.05$). Lung density histograms of 5 COVID+ patients with high elastance (type H) were similar to those of COVID− patients, while those of the 8 COVID+ patients with normal elastance (type L) displayed higher aerated lung fraction.

1. Introduction

COVID-19 has emerged as a major public health problem, with a death toll amounting to several hundred thousand worldwide during the first months since epidemic onset. 14 to 26% of hospitalized patients for COVID-19 require intensive admission in intensive care units (ICU) [1,2], and preliminary reports suggest that ICU mortality is high in patients under invasive mechanical ventilation [1-3]. Duration of invasive mechanical ventilation in ICU survivors exceed 10 days [4], and virtually all patients under invasive mechanical ventilation fulfill acute respiratory syndrome (ARDS) criteria [5]. However, based on remarkably preserved lung elastance and evidence of high shunt fraction in 16 patients, it was hypothesized that COVID-19 does not lead to a "typical" ARDS [6]. The same author reported that 70–80% of the patients in his center presented with normal lung elastance (type L) (suggesting that the amount of gas in the lung is nearly normal in this group of patients [7]), and 20–30% presented with high elastance (type H) [8]. The consequence of this is crucial for mechanical ventilation management, as this would preclude the use of high positive end-expiratory pressure (PEEP) levels in the majority of COVID-19 ARDS patients.

Computed tomography (CT) is an appealing tool to explore COVID-19 ARDS, as it provides information on spatial heterogeneity of ARDS lesions and allows regional analyses of tidal recruitment and hyperinflation, both being related to impaired ARDS outcome [9,10].

The aim of this study was 1- to assess with CT whether lung weight and aeration of COVID-19 (COVID+) ARDS differ from those of non-COVID-19 (COVID−) ARDS; 2- to compare the amount of tidal hyperinflation and recruitment in both groups of patients.

2. Material and methods

2.1. Study design and setting

The study is an ancillary study of an ongoing single-center prospective observational study performed in an ICU of a university hospital, aiming to validate a semi-automatic software for lung segmentation with CT. The trial was registered at ClinicalTrials.gov (NCT03870009) and the protocol approved by an ethics committee (CPP-Ouest3-

* Corresponding author at: Service de Réanimation Médicale, 103 Grande Rue de la Croix Rousse, 69004 Lyon, France.
E-mail address: j-christophe.richard@chu-lyon.fr (J.-C. Richard).

https://doi.org/10.1016/j.jcrc.2020.08.006
0883-9441/

IRB2019-A00024-53). Patients were enrolled between May 2019 and May 2020.

2.2. Patients

Eligible participants were aged 18 years or older, under invasive mechanical ventilation, with ARDS [11] and a $PaO_2/FiO_2 \leq 200$ mmHg, already implanted with an esophageal catheter, and had an indication for CT.

Exclusion criteria were ARDS onset >72 h, requirement for contrast agent injection during CT, chronic obstructive pulmonary disease, pneumothorax, contra-indication to the transport to the imaging facility ($PaO_2/FIO_2 < 60$ Torr, mean arterial pressure <65 mmHg, or intracranial hypertension), patient under any extracorporeal oxygenation technique, previous inclusion in present study, advanced directives to withhold or withdraw life-sustaining treatment, pregnancy, exclusion period related to inclusion in another clinical trial, patient under a legal protective measure, lack of affiliation to social security, lack of informed consent by patient's relative.

2.3. Protocol description

Optimal inflated volume identification and placement of the esophageal balloon (C7680U-Marquat, Boissy-St-Leger, France) was performed as recommended [12]. Patients were ventilated with tidal volume (VT) 6 ml/kg of predicted body weight, and PEEP set using a PEEP-FiO_2 table [13]. Respiratory measurements and arterial blood gas were performed 1 h after adjustment of ventilatory settings. Patients were transferred to the imaging facility using their ICU ventilator to avoid patient-ventilator disconnection. However, 7 patients were transferred using a transport ventilator (ELYSEE 150 -Air Liquide Medical Systems, Antony, France) because of excessive workload during COVID-19 epidemic. They were switched back to their ICU ventilator before CT acquisition. The endotracheal tube was transiently occluded with a Kocher clamp during each ventilator change to avoid derecruitment. Ventilator settings were kept unchanged during transport and imaging.

2.4. Data collection

The following variables were recorded at inclusion: demographic and anthropometric data, time of ARDS identification, ARDS severity and risk factors, SAPS2 [14] and SOFA [15] scores, ventilatory settings, and arterial blood gas.

2.5. Measurements

Total PEEP of the respiratory system ($PEEP_{tot,rs}$), plateau pressure of the respiratory system ($P_{Plat,rs}$), end-expiratory and end-inspiratory esophageal pressures were measured at the end of 3-s end-expiratory and end-inspiratory pauses. Transpulmonary total PEEP ($PEEP_{tot,L}$) and transpulmonary plateau pressure ($P_{plat,L}$) were computed as airway pressures minus esophageal pressures. Airway driving pressure (ΔP_{rs}) and transpulmonary driving pressure (ΔP_L) were computed as $P_{Plat,rs}$ minus $PEEP_{tot,rs}$, and $P_{Plat,L}$ minus $PEEP_{tot,L}$, respectively. Respiratory system (E_{rs}) and lung (E_L) elastances were computed as ΔP_{rs} and ΔP_L divided by VT, respectively. Elastance-derived end-inspiratory transpulmonary pressure (TPP_{EI}) was calculated as $P_{plat,rs} \times E_L/E_{rs}$. COVID+ patients with $E_{rs} > 20$ cm $H_2O.L^{-1}$ were classified as type H patients, and those with $E_{rs} \leq 20$ cm $H_2O.L^{-1}$ as type L, as recently proposed [16].

Theoretical lung weight was computed as follows [17]: lung weight (g) = $-1806.1 + 1633.7 \times$ subject's height (m).

2.6. CT measurements

CT acquisitions were performed in the supine position with an iCT 256 or Ingenuity CT (Philips Healthcare, Eindhoven, The Netherlands) using the following settings: voltage 140 kVP, slice thickness 1 mm, matrix size 512 × 512. Field of view, pixel size and mAs were adapted for each patient.

Lung scanning was performed from apex to base during both end-expiratory and end-inspiratory pauses, and lack of respiratory efforts during the pause was visually checked on the ventilator pressure-time curves. Image reconstruction was performed using a smooth filter (kernel B). The lungs were manually segmented by some of the authors (FD, LC, JCR) with a CreaTools-based software [18], excluding pleural effusions, hilar and mediastinal structures. Segmented lung volumes were analyzed using MATLAB (MathWorks, Natick, MA).

Tissue and gas fraction were computed as follows [7]:

- Tissue fraction = 1 − CT number/−1000
- Gas fraction = CT number/−1000

Tissue and gas volume were computed as the product of tissue and gas fractions with voxel volume, respectively.

2.7. CT analyses on the whole lung

Lung parenchyma was then classified into four compartments, according to CT number: noninflated (density between +100 and −100 Hounsfield units (HU)), poorly inflated (density between −101 and −500 HU), normally inflated (density between −501 and −900 HU), and overinflated tissue (density between −901 and −1,000 HU). The volume of each compartment was measured at end-expiration and end-inspiration. Total lung weight and weight of each compartment was estimated using lung tissue volume, assuming a tissue density of 1 $g.ml^{-1}$ [19].

Tidal hyperinflation was defined as the volume of the overinflated compartment at end-inspiration minus the volume of the overinflated compartment at end-expiration [9]. Tidal recruitment of the noninflated compartment and of the poorly inflated compartment were defined as the volume of the noninflated and poorly inflated compartments at end-expiration minus their volumes at end-inspiration [9], respectively. They were expressed as a percentage of the tidal inflation–related change in CT lung aeration.

2.8. Regional CT analyses

Both lungs were divided into 10 sections along the apico-caudal dimension. Each section was divided into 10 ventro-dorsal levels of equal height [20]. Level 1 refers to the most ventral region, while level 10 refers to the most dorsal. The height of each level was measured as the distance from the most ventral to the most dorsal surface of the level in examination. The hydrostatic pressure of each level [20] was then computed as:

Hydrostatic pressure = (1-CT number)/−1000 × h, with h being the height of the level.

The superimposed pressure on a given level was defined in each lung as the sum of the pressure of the level plus the pressures of the levels above. The total superimposed pressure was defined as the superimposed pressure in the most dorsal level, i.e., level 10.

2.9. Statistical analysis

Statistical analysis was performed using R with packages PropCIs [21], emmeans [22], Lme4 [23], lmerTest [24], boot [25,26] and gamm4 [27]. A *p*-value below 0.05 was chosen for statistical significance.

Data were expressed as mean ± standard deviation. 95% confidence intervals ($CI_{95\%}$) of quantitative variables were computed with the bias corrected and accelerated-bootstrap method with 10,000 replicates [28]. $CI_{95\%}$ of proportions were computed with the Wilson score method. Data were compared between groups with the Fisher's exact test for categorical variables and *t*-test, Mann-Whitney *U* test or

ANOVA for continuous variables. Comparison between the mean of a quantitative variable and a theoretical mean was performed using one-sample t-test. Correlations between variables were assessed with the Pearson method. The weight of each compartment was compared between groups by a linear mixed model using COVID status, respiratory phase (inspiration and expiration) and compartment as fixed effects, and patient as random intercept. Interactions were analyzed by testing contrasts on estimated marginal means. Lung voxels were classified in 11 intervals of equal size between −1000 and + 100 HU as a function of their CT-density. Voxel number in each compartment was expressed as a percentage of lung volume and fitted using a generalized additive mixed model using COVID-19 status, HU interval and their interaction as fixed effects, HU interval as random slope and patient as random intercept. Regional analyses of CT parameters were performed with linear mixed models using COVID-19 status and lung level with their interaction as fixed effects and patient as random effect. Estimation of sample size was not computed as the study is exploratory, and data collection stopped with the control of COVID-19 epidemic in our area.

3. Results

3.1. Characteristics at inclusion

23 patients were included, of whom 13 presented with COVID + ARDS. Reasons for non-inclusion are listed in Supplementary material 1. Patients characteristics at inclusion are reported in Table 1.

3.2. Physiological variables

Respiratory mechanics and arterial blood gas are reported Table 2. PEEP, VT, and respiratory rate were not significantly different between COVID+ and COVID− patients. Five (38%) of the COVID+ patients presented with abnormally elevated elastance of the respiratory system, as compared to 8 (80%) of the COVID− patients ($p = 0.09$). E_L was significantly lower in COVID+ patients 14 ± 6 vs. 22 ± 8 cm $H_2O.L^{-1}$, $p < 0.05$). Consequently, end-inspiratory TPP_{EI} was significantly lower in COVID+ patients (13 ± 4 vs. 17 ± 3 cm H_2O, $p < 0.05$).

3.3. Global analysis of CT-derived variables

CT scan was performed 48 ± 25 min after respiratory mechanics assessment. Lung weight normalized to theoretical lung weight was significantly higher in COVID− ARDS patients (195 ± 46% [$CI_{95\%}$: 172–226%] vs. 163 ± 26% [$CI_{95\%}$: 149–176%], $p < 0.05$, Fig. 1). All COVID+ patients presented supranormal lung weight values ($p < 0.05$ for the comparison with theoretical normal lung weight). Tidal recruitment of the noninflated compartment was significantly higher in COVID− ARDS (20 ± 12 vs. 9 ± 11% of VT, $p < 0.05$). Tidal hyperinflation was greater than 20% of the VT in 6 (46%) COVID+ and 3 (30%) COVID− patients.

Noninflated tissue was significantly higher in COVID− patients (36 ± 14% vs. 26 ± 15% of total lung weight), while normally inflated tissue was significantly lower (27 ± 12% vs. 35 ± 14% of total lung weight), as compared to COVID+ patients (Fig. 2).

Correlation matrix of respiratory mechanics, blood gas and CT variables is presented in Supplementary material 2. The only significant association between respiratory mechanics and CT-derived variables was a positive correlation between PEEP and tidal hyperinflation.

3.4. Regional analyses of CT-derived variables

Regional superimposed pressure increased significantly more from level 1 to level 10 in COVID− ARDS patients ($p < 0.05$ for interaction, Supplementary material 3). However, the total superimposed pressure was not significantly different in COVID− and COVID+ patients (9 ± 2 vs. 8 ± 1 cm H_2O, $p = 0.27$).

Table 1
Characteristics on the day of inclusion.

Variables	Whole dataset	COVID− ($n = 10$)	COVID+ ($n = 13$)
Sex male	20 (87%)	8 (80%)	12 (92%)
Age (yr)	62 ± 15	60 ± 15	64 ± 15
Height (cm)	170 ± 11	170 ± 14	170 ± 9
BMI ($kg.m^{-2}$)	30 ± 6	30 ± 8	29 ± 5
Delay between ICU admission and inclusion (day)	2 ± 2	2 ± 2	2 ± 2
Delay between inclusion and ARDS onset (day)	1 ± 1	1 ± 1	1 ± 1
SAPS 2 at ICU admission	42 ± 15	49 ± 18	38 ± 12
SOFA score at inclusion	12 ± 3	13 ± 3	11 ± 2[a]
ARDS risk factor			
• pneumonia	20 (87%)	7 (70%)	13 (100%)
• aspiration	3 (13%)	3 (30%)	0 (0%)
ARDS severity			
• moderate	12 (52%)	3 (30%)	9 (69%)
• severe	11 (48%)	7 (70%)	4 (31%)
Prone position	15 (65%)	7 (70%)	8 (62%)
NMBA	23 (100%)	10 (100%)	13 (100%)
RRT	0 (0%)	0 (0%)	0 (0%)
Inotropes administration	0 (0%)	0 (0%)	0 (0%)
Vasopressor administration	19 (83%)	8 (80%)	11 (85%)

Values are mean ± standard deviation or count (percentage).
ARDS = acute respiratory distress syndrome; BMI = body mass index; COVID− = non-COVID-19 ARDS patients; COVID+ = COVID-19 ARDS patients; ICU = intensive care unit; NMBA = neuromuscular blocking agents; RRT = renal replacement therapy; SAPS2 = simplified acute physiology score.
[a] $p < 0.05$ between groups.

Table 2
Respiratory mechanics and arterial blood gas.

Variables	COVID− ($n = 10$)	COVID+ ($n = 13$)
PEEP (cm H_2O)	9 ± 3	11 ± 2
VT ($ml.kg^{-1}$ PBW)	6.0 ± 0.2	6.0 ± 0.0
RR (min^{-1})	25 ± 5	23 ± 3
Ti/Ttotal (%)	33 ± 1	32 ± 2
$PEEP_{tot,rs}$ (cm H_2O)	11 ± 3	12 ± 2
$P_{plat,rs}$ (cm H_2O)	21 ± 2	20 ± 3
ΔP_{rs} (cm H_2O)	10 ± 3	8 ± 2[a]
ΔP_L (cm H_2O)	8 ± 2	5 ± 2[a]
E_{rs} (cm $H_2O.L^{-1}$)	28 ± 13	21 ± 7
$E_{rs} > 20$ cm $H_2O.L^{-1}$	8 (80%)	5 (38%)
E_L (cm $H_2O.L^{-1}$)	22 ± 8	14 ± 6[a]
E_{cw} (cm $H_2O.L^{-1}$)	6 ± 5	7 ± 3
E_L/E_{rs} (%)	81 ± 11	65 ± 14[a]
End-inspiratory TPP_{EI}	17 ± 3	13 ± 4[a]
pH	7.34 ± 0.09	7.36 ± 0.10
PaO_2/FiO_2 (Torr)	122 ± 41	130 ± 28
$PaCO_2$ (Torr)	48 ± 8	46 ± 8
Bicarbonates ($mmol.L^{-1}$)	25 ± 6	26 ± 4
Lactate ($mmol.L^{-1}$)	4.8 ± 4.4	1.8 ± 0.5[a]

Values are mean ± standard deviation or count(percentage).
COVID− = non-COVID-19 ARDS patients; COVID+ = COVID-19 ARDS patients; ΔP_{rs} = driving pressure of the respiratory system; ΔP_L = transpulmonary driving pressure; E_{cw} = chest wall elastance; E_L = lung elastance; E_{rs} = elastance of the respiratory system; FiO_2 = inspired fraction of oxygen; PaO_2 = oxygen partial pressure in arterial blood; $PaCO_2$ = carbo dioxide partial pressure in arterial blood; PBW = predicted body weight; PEEP = positive end-expiratory pressure; $PEEP_{tot,rs}$ = total PEEP of the respiratory system; $P_{plat,rs}$ = plateau pressure of the respiratory system; RR = respiratory rate; Ti/Ttotal = ratio of inspiratory time over total time of the respiratory cycle; TPP_{EI} = elastance-derived transpulmonary pressure; VT = tidal volume.
[a] $p < 0.05$ between groups.

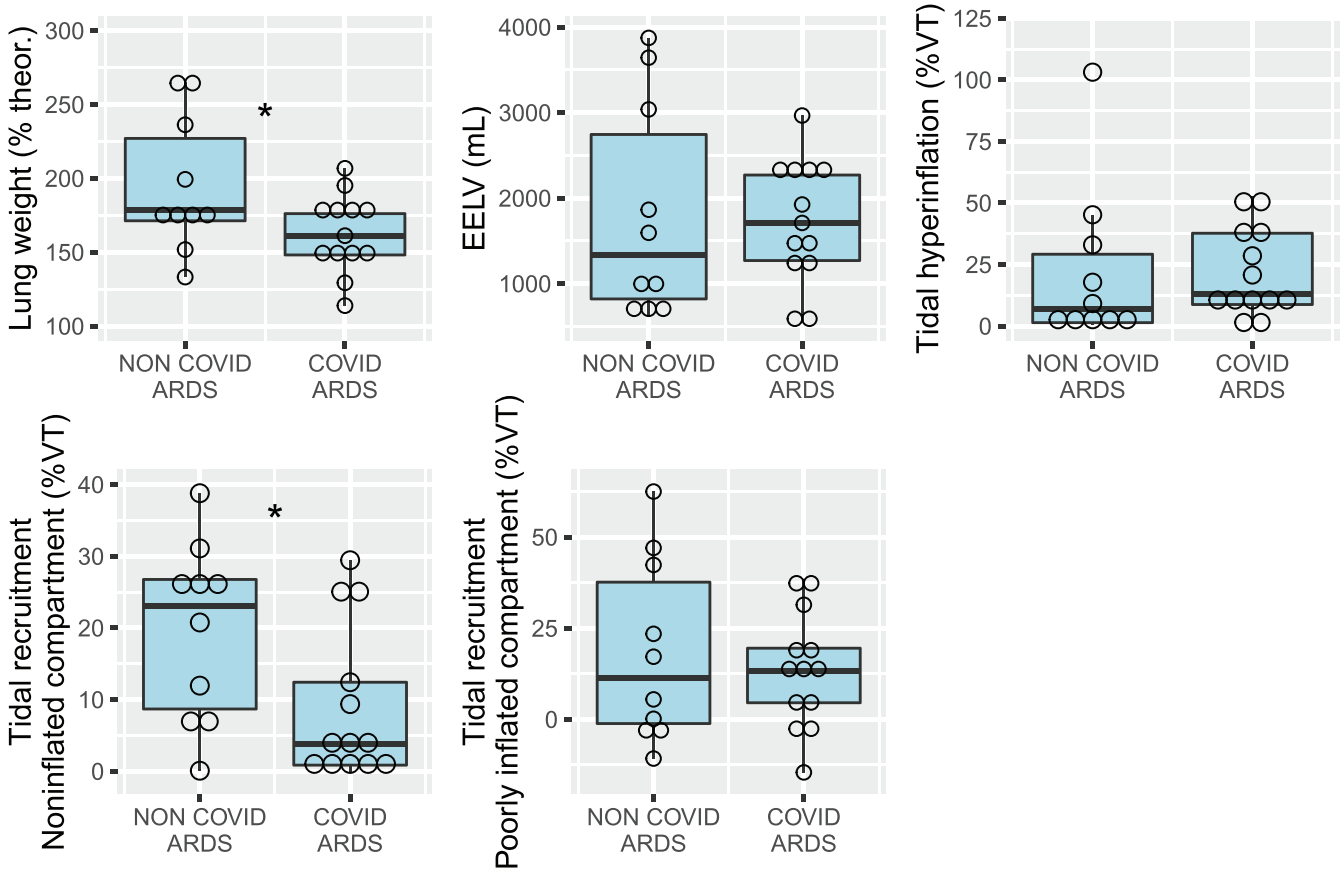

Fig. 1. CT measurements in non-COVID-19 and COVID-19 ARDS patients. ARDS = acute respiratory distress syndrome; CT = computed tomography; EELV = end-expiratory aerated lung volume; theor = theoretical lung weight; VT = CT-derived tidal volume. Open circles are individual datapoints. *$p < 0.05$ between groups.

3.5. Supplementary analyses based on COVID subtype

According to their E_{rs}, 5 COVID+ patients (38% [$CI_{95\%}$: 18%–54%] were classified as type H and 8 (62% [$CI_{95\%}$: 36%–82%] as type L. Respiratory, blood gas and CT variables as a function of COVID-19 subtypes are presented in Supplementary material 4. ARDS severity, $P_{plat,rs}$, ΔP_{rs}, ΔP_L, and noninflated compartment at end-expiration were lower in the L subtype, while normally inflated compartment at end-expiration was significantly higher.

Representative CT scans of 3 patients are presented Fig. 3. On lung density histograms, type H and COVID− patients presented with similar patterns (Fig. 4), while type L patients presented with higher percentage of lung volume within the normal inflation rage and lower in the non-inflation range, as shown by a clear separation of the 95% confidence interval of the fitted values per group.

4. Discussion

The main findings of the study are the following: 1- lung weight is significantly increased in all COVID+ ARDS patients as compared to normal values, although significantly lower than in COVID− ARDS; 2- tidal recruitment and non-inflated lung volume are significantly lower in COVID+ ARDS patients suggesting that lung potential for recruitment may be lower in this group; 3-a substantial proportion of COVID+ ARDS patients exhibit large amount of tidal hyperinflation, suggesting that PEEP level and/or tidal volume may be excessive, despite plateau pressure and driving pressure within acceptable range.

4.1. Respiratory mechanics and blood gas

The study identified near-normal respiratory system elastance in 62% of the COVID+ patients at the early phase of ARDS, in keeping with a previous report [8]. Therefore, lung elastance was significantly lower in COVID+ patients, suggesting that response to PEEP increase would mainly increase aeration of normally inflated lung regions. However, PEEP and PaO_2/FiO_2 ratio were similar in both group of patients, since a PEEP-FiO_2 table to standardize ventilation parameters. As the amount of noninflated lung was significantly higher in COVID− patients with similar oxygenation, it may be hypothesized that ventilation-perfusion mismatch may be greater in this group as a possible consequence of the endothelial tropism of SARS-CoV2 [29]. This relative discrepancy between arterial oxygenation and the amount of non-inflated lung was also identified previously [8].

4.2. CT data

Scarce data have been published to date on quantitative CT features in COVID+ ARDS patients. On 2 COVID+ ARDS patients, Gattinoni et al. identified one pattern with near normal lung weight, low non-inflated tissue volume, high venous admixture and normal respiratory system elastance, and one pattern with increased lung weight, high percentage of non-inflated tissue, high venous admixture and high elastance [16]. In the present study, we demonstrate a substantial increase in lung weight in all COVID+ patients as compared to theoretical value, suggesting that these patients exhibited either lung edema and/or an increase in lung blood volume, as it is unlikely that inflammatory cells

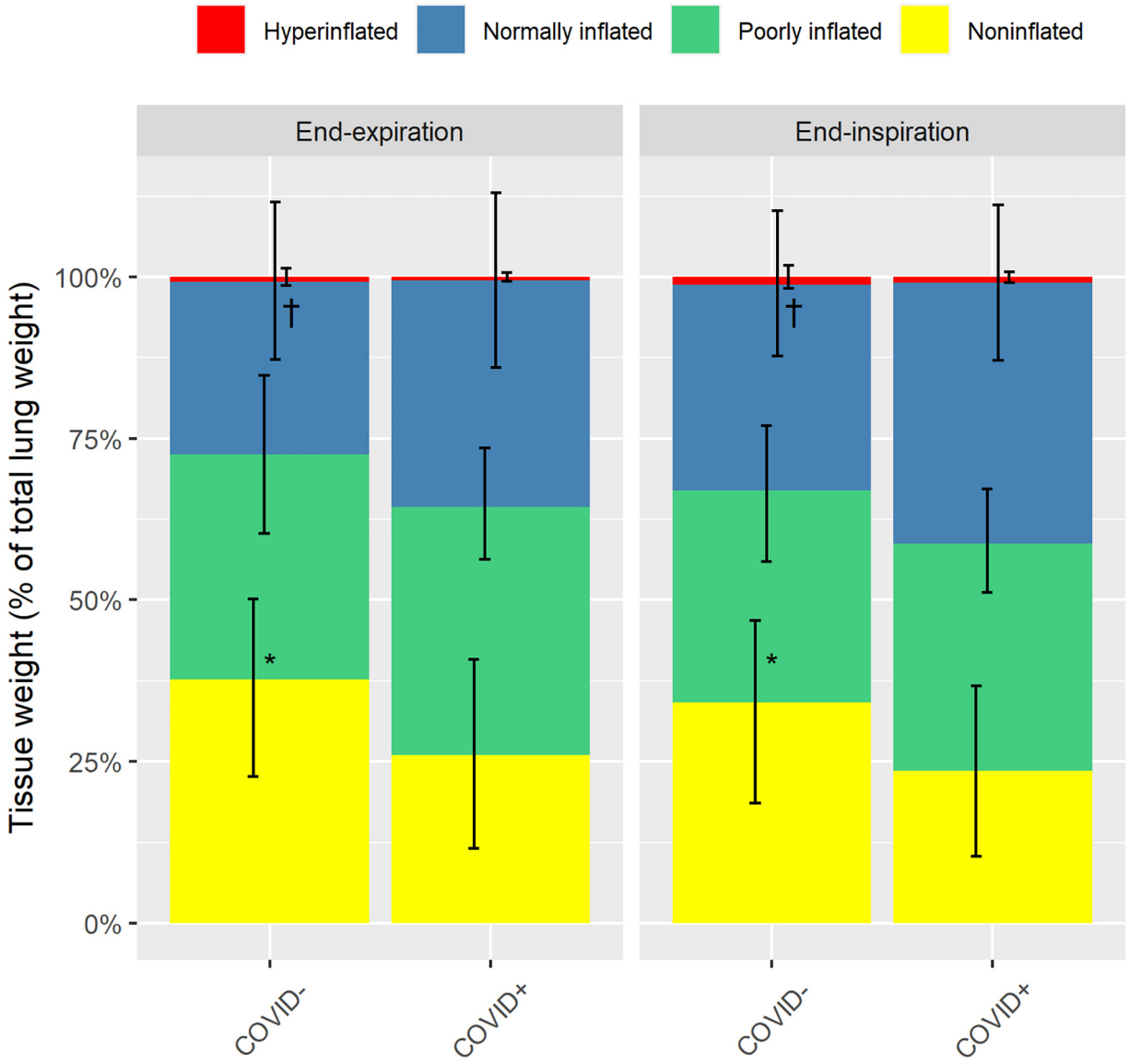

Fig. 2. Proportion of total lung tissue classified according to the level of inflation. Values are provided at both end-expiration and end-inspiration in COVID-19 ARDS patients (COVID+) and non-COVID-19 ARDS patients (COVID−). Yellow, green, blue and red bars refer to noninflated, poorly inflated, normally inflated, and overinflated lung tissue, respectively. Error bars are standard deviations. *$p < 0.01$ for noninflated tissue between COVID+ and COVID− patients. †$p < 0.05$ for normally inflated tissue between COVID+ and COVID− patients.

alone could achieve such an increase in lung weight. Furthermore, while the amount of noninflated lung (26% of total lung weight) was significantly lower in COVID+ patients as compared to COVID− patients in the present study, this amount was similar to ARDS with low recruitment potential in the study of Gattinoni et al. [30].

As tidal recruitment was significantly lower in COVID+ patients (i.e. increased pressure over PEEP level related to tidal inflation does not lead to substantial recruitment in these patients), it may be hypothesized that these patients present a low potential for recruitment. Indeed, Caironi et al. have shown that tidal recruitment is lower in patients with lower recruitment potential, while patients with high recruitment potential presented high fractions of lung volume with tidal recruitment [10]. The lower amount of non-inflated lung tissue in COVID+ patients is in accordance with this hypothesis. However, using tidal recruitment to infer on recruitment potential is only speculative, as we did not specifically measure recruitment potential in the present study. Furthermore, as superimposed pressure was substantially increased in COVID+ patients as compared to normal values (2.6 ± 0.5 cm H_2O [17]), this suggest that a minimal amount of PEEP is required to counteract gravitational forces and maintain arterial oxygenation within acceptable range.

We observed that tidal hyperinflation was greater than 20% in more than 30% of both COVID+ and COVID− ARDS patients, a rate similar to previously published data on COVID− ARDS patients [9]. While existence of a safety threshold regarding this parameter is currently unknown, it was previously shown that tidal hyperinflation is independently related to ARDS prognosis [9,10], and that a subgroup of ARDS patients with impaired prognosis presented with tidal hyperinflation greater than 20% of the VT [9]. It may be hypothesized that PEEP and/or VT may be excessive in this subgroup of patients, although plateau pressure, driving pressure and TPP_{EI} were kept within acceptable range.

Finally, we observed that a subtype of COVID+ ARDS patients with high elastance has similar CT features than COVID− ARDS, suggesting that their ventilatory management should be similar. To the opposite, the subtype of COVID+ with low elastance has low tidal recruitment, lower amount of non-inflated lung (i.e. derecruited lung potentially re-

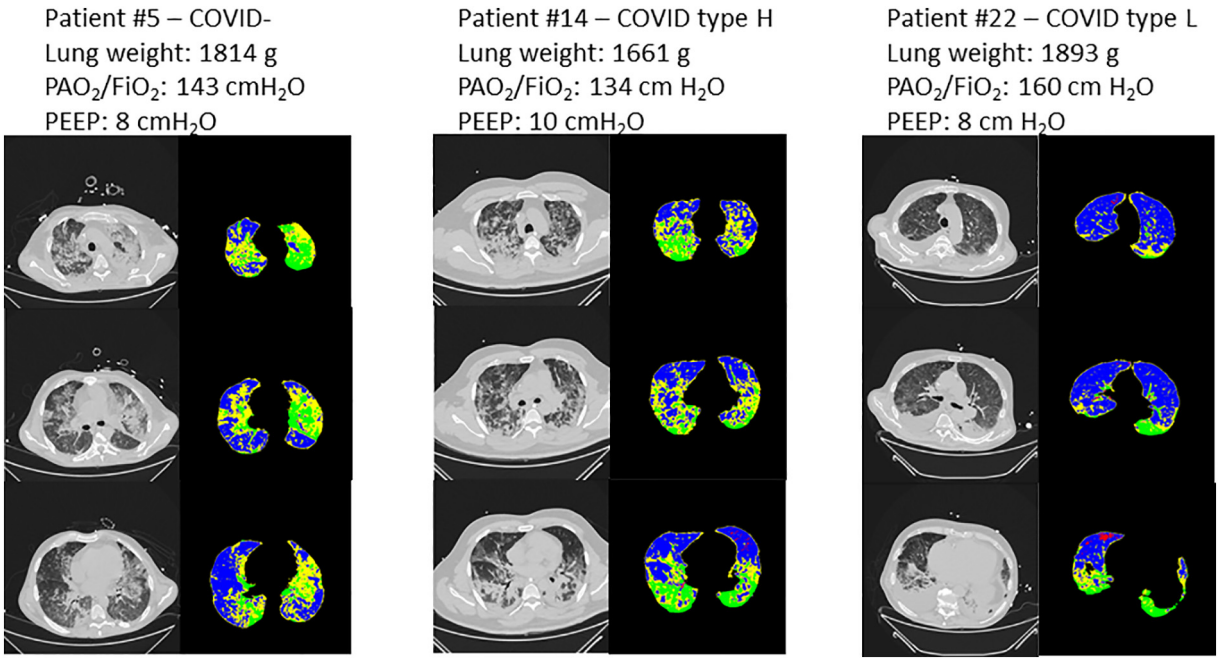

Fig. 3. Representative CT scans of 3 patients. Left panel: patient with non-COVID-19 ARDS; middle panel: type-H COVID-19 ARDS patient; right panel: type-L COVID-19 ARDS patient. For each patient, 3 CT slices are presented at the level of the aortic arch (top panel), the main bronchi division (middle panel) and immediately above the right diaphragmatic dome (bottom panel). At each level, a grey colour scale is presented as well as the corresponding parametric CT with red representing overinflated voxels, blue normally inflated voxels, yellow poorly aerated voxels, and green nonaerated voxels. Lung weight assessed on CT, PaO_2/FiO_2 ratio and PEEP level are provided for each patient on top of their corresponding CT images.

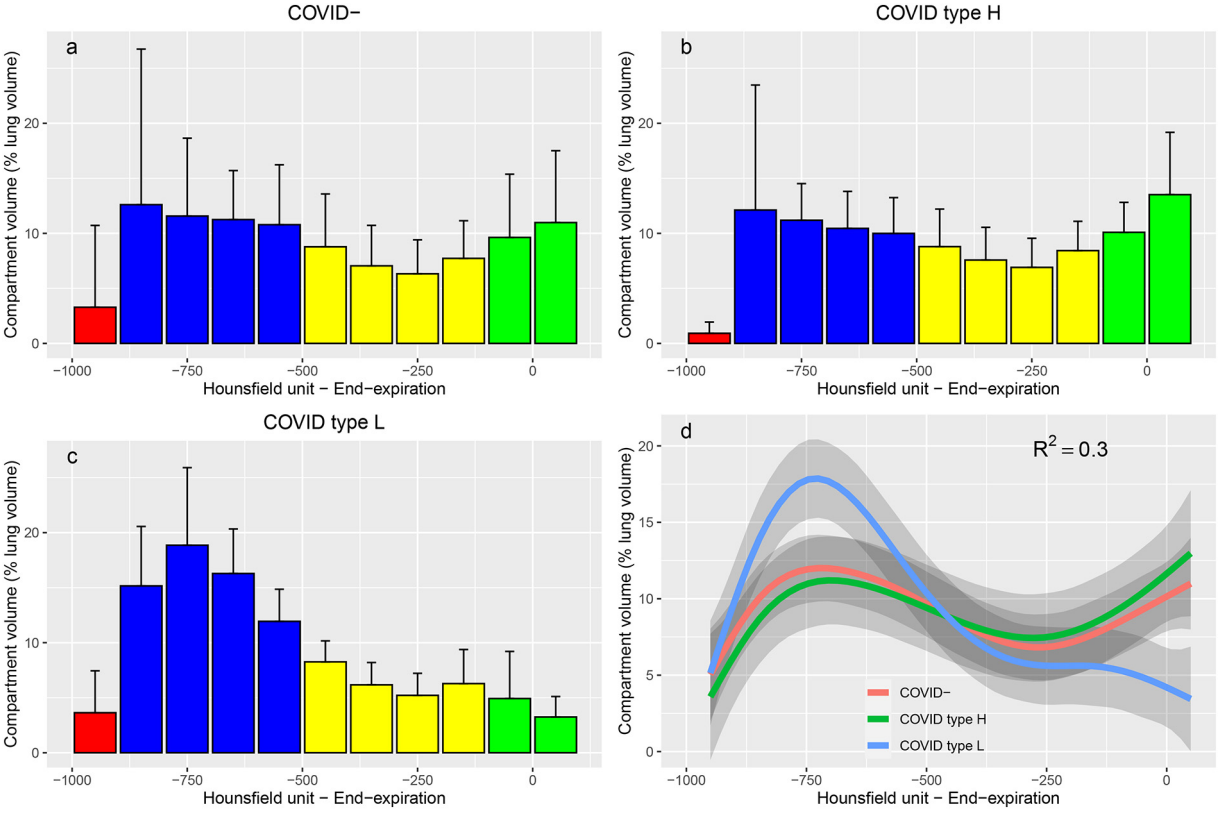

Fig. 4. Lung density histograms. Value are provided for COVID− ($n = 10$ patients, panel a), type H ($n = 5$ patients, panel b) and type L ($n = 8$ patients, panel c) ARDS patients. Histograms represents the volume of all the voxels belonging to each interval of 100 Hounsfield units width, normalized by total lung volume. Bars are mean values and error bars are standard deviations. Red bars represent intervals within the over inflation range, blue bars intervals within the normal inflation range, yellow intervals within the poor inflation range, and green intervals within the non-aeration range. Panel d represent the fitted values in each group, with R^2 of the general additive mixed model (red, green and blue lines refer to COVID −, Type H and type L groups, respectively). Grey shade areas represent 95% confidence interval of the fitted values.

aerated by PEEP increase), higher normally inflated lung compartment, and should respond to higher PEEP by an increase in normally and over-inflated lung, without significant recruitment of nonaerated lung.

4.3. Strengths and limits

Some limitations of the present study should be acknowledged. First, the small sample size limits the generalizability of the results. This small sample size makes the study underpowered to detect small differences between COVID+ and COVID− patients, or between type H and type L subtypes. Second, the use of a transport ventilator in 7 patients of the study may have promoted alveolar derecruitment, although this was prevented by clamping of the tracheal tube during ventilator change. Third, a major limitation of the study is that potential for recruitment could not be assessed as CT acquisition at both low and high PEEP were not performed to minimize radiation exposure. Fourth, as contrast agents injection was not used for CT acquisition to avoid bias in measured gas and tissue fractions [31], we cannot rule out pulmonary embolism as a potential factor implicated in hypoxemia. Five, owing to well-known limitations of the current ARDS definition [32], it is virtually impossible to confirm that all included patients presented with permeability type pulmonary edema, although this would apply to both COVID + and COVID− ARDS patients.

Nevertheless, this study is the first CT scan study with quantitative analysis on a small cohort of COVID+ ARDS patients. CT acquisitions were performed early, mostly within 1 day of ARDS onset, thus minimizing potential confounding effects related to ventilator-induced lung injury or ventilator-associated pneumonia.

5. Conclusion

COVID+ ARDS patients share similar CT features with COVID - patients (increased lung weight, increased noninflated lung fraction). A subtype of COVID-19 ARDS patients with near-normal elastance present with low tidal recruitment, low amount of non-inflated lung, and high amount of normally aerated lung, questioning the relevance of high PEEP levels in this subgroup.

Supplementary data to this article can be found online at https://doi.org/10.1016/j.jcrc.2020.08.006.

Funding

This work was performed within the framework of the LABEX PRIMES (ANR-11-LABX-0063) of Université de Lyon, within the program "Investissements d'Avenir" (ANR-11-IDEX-0007) operated by the French National Research Agency (ANR).

Insurance and quality monitoring for the study were funded by Hospices Civils de Lyon.

Financial disclosure statement

None.

Declaration of Competing Interest

The authors declare that they have no conflict of interest.

Acknowledgements

The authors wish to thank Loredana Baboi for her help with inclusion of the patients in the study and data acquisition.

References

[1] Richardson S, Hirsch JS, Narasimhan M, Crawford JM, McGinn T, Davidson KW, et al. Presenting characteristics, comorbidities, and outcomes among 5700 patients hospitalized with COVID-19 in the New York city area. JAMA 2020. https://doi.org/10.1001/jama.2020.6775.
[2] Wu C, Chen X, Cai Y, Xia J, Zhou X, Xu S, et al. Risk factors associated with acute respiratory distress syndrome and death in patients with coronavirus disease 2019 pneumonia in Wuhan, China. JAMA Intern Med 2020. https://doi.org/10.1001/jamainternmed.2020.0994.
[3] Grasselli G, Zangrillo A, Zanella A, Antonelli M, Cabrini L, Castelli A, et al. Baseline characteristics and outcomes of 1591 patients infected with SARS-CoV-2 admitted to ICUs of the Lombardy Region, Italy. JAMA 2020;323:1574–81. https://doi.org/10.1001/jama.2020.5394.
[4] Bhatraju PK, Ghassemieh BJ, Nichols M, Kim R, Jerome KR, Nalla AK, et al. Covid-19 in critically ill patients in the Seattle region - case series. N Engl J Med 2020;382:2012–22. https://doi.org/10.1056/NEJMoa2004500.
[5] Arentz M, Yim E, Klaff L, Lokhandwala S, Riedo FX, Chong M, et al. Characteristics and outcomes of 21 critically ill patients with COVID-19 in Washington state. JAMA 2020;323:1612–4. https://doi.org/10.1001/jama.2020.4326.
[6] Gattinoni L, Coppola S, Cressoni M, Busana M, Rossi S, Chiumello D. Covid-19 does not lead to a "typical" acute respiratory distress syndrome. Am J Respir Crit Care Med 2020;201:1299–300. https://doi.org/10.1164/rccm.202003-0817LE.
[7] Gattinoni L, Pesenti A, Avalli L, Rossi F, Bombino M. Pressure-volume curve of total respiratory system in acute respiratory failure. Computed tomographic scan study. Am Rev Respir Dis 1987;136:730–6. https://doi.org/10.1164/ajrccm/136.3.730.
[8] Gattinoni L, Chiumello D, Caironi P, Busana M, Romitti F, Brazzi L, et al. COVID-19 pneumonia: different respiratory treatments for different phenotypes? Intensive Care Med 2020. https://doi.org/10.1007/s00134-020-06033-2.
[9] Terragni PP, Rosboch G, Tealdi A, Corno E, Menaldo E, Davini O, et al. Tidal hyperinflation during low tidal volume ventilation in acute respiratory distress syndrome. Am J Respir Crit Care Med 2007;175:160–6. https://doi.org/10.1164/rccm.200607-915OC.
[10] Caironi P, Cressoni M, Chiumello D, Ranieri M, Quintel M, Russo SG, et al. Lung opening and closing during ventilation of acute respiratory distress syndrome. Am J Respir Crit Care Med 2010;181:578–86. https://doi.org/10.1164/rccm.200905-0787OC.
[11] Definition Task Force ARDS, Ranieri VM, Rubenfeld GD, Thompson BT, Ferguson ND, Caldwell E, et al. Acute respiratory distress syndrome: the Berlin Definition. JAMA 2012;307:2526–33. https://doi.org/10.1001/jama.2012.5669.
[12] Akoumianaki E, Maggiore SM, Valenza F, Bellani G, Jubran A, Loring SH, et al. The application of esophageal pressure measurement in patients with respiratory failure. Am J Respir Crit Care Med 2014;189:520–31. https://doi.org/10.1164/rccm.201312-2193CI.
[13] Network Acute Respiratory Distress Syndrome, Brower RG, Matthay MA, Morris A, Schoenfeld D, Thompson BT, et al. Ventilation with lower tidal volumes as compared with traditional tidal volumes for acute lung injury and the acute respiratory distress syndrome. N Engl J Med 2000;342:1301–8. https://doi.org/10.1056/NEJM200005043421801.
[14] Le Gall JR, Lemeshow S, Saulnier F. A new Simplified Acute Physiology Score (SAPS II) based on a European/North American multicenter study. JAMA 1993;270:2957–63. https://doi.org/10.1001/jama.1993.03510240069035.
[15] Vincent JL, Moreno R, Takala J, Willatts S, De Mendonca A, Bruining H, et al. The SOFA (Sepsis-related Organ Failure Assessment) score to describe organ dysfunction/failure. On behalf of the Working Group on Sepsis-Related Problems of the European Society of Intensive Care Medicine. Intensive Care Med 1996;22:707–10.
[16] Gattinoni L, Chiumello D, Rossi S. COVID-19 pneumonia: ARDS or not? Crit Care 2020;24:154. https://doi.org/10.1186/s13054-020-02880-z.
[17] Cressoni M, Gallazzi E, Chiurazzi C, Marino A, Brioni M, Menga F, et al. Limits of normality of quantitative thoracic CT analysis. Crit Care 2013;17:R93. https://doi.org/10.1186/cc12738.
[18] Dávila-Serrano EE, Guigues L, Cervenansky F, Pop S, Riveros Reyes JG, Flórez-Valencia L, et al. CreaTools: a framework to develop medical image processing software. Application to simulate pipeline stent deployment in intracranial vessels with aneurysms. Computer vision and graphics, ICCVG 2012, lecture notes in computer science. , vol. 7594Berlin Heidelberg: Springer; 2012; 55–62.
[19] Gattinoni L, Pesenti A, Bombino M, Baglioni S, Rivolta M, Rossi F, et al. Relationships between lung computed tomographic density, gas exchange, and PEEP in acute respiratory failure. Anesthesiology 1988;69:824–32. https://doi.org/10.1097/00000542-198812000-00005.
[20] Pelosi P, D'Andrea L, Vitale G, Pesenti A, Gattinoni L. Vertical gradient of regional lung inflation in adult respiratory distress syndrome. Am J Respir Crit Care Med 1994;149:8–13.
[21] Scherer R. PropCIs: various confidence interval methods for proportions; 2018.
[22] Lenth R. emmeans: estimated marginal means, aka least-squares means; 2019.
[23] Bates D, Maechler M, Bolker B, Walker S. Fitting linear mixed-effects models using lme4. J Stat Softw 2015;67:1–48. https://doi.org/10.18637/jss.v067.i01.
[24] Kuznetsova A, Brockhoff PB, Christensen RHB. lmerTest package: tests in linear mixed effects models. J Stat Softw 2017;82:1–26. https://doi.org/10.18637/jss.v082.i13.
[25] Canty A, Ripley B. Boot: bootstrap R (S-Plus) functions; 2020.
[26] Davison AC, Hinkley DV. Bootstrap Methods and Their Applications. Cambridge: Cambridge University Press; 1997.
[27] Wood S, Scheipel F. gamm4: generalized additive mixed models using "mgcv" and "lme4"; 2020.
[28] Efron B. Better bootstrap confidence intervals. J Am Stat Assoc 1987;82:171–85.
[29] Varga Z, Flammer AJ, Steiger P, Haberecker M, Andermatt R, Zinkernagel AS, et al. Endothelial cell infection and endotheliitis in COVID-19. Lancet 2020;395:1417–8. https://doi.org/10.1016/S0140-6736(20)30937-5.

[30] Gattinoni L, Caironi P, Cressoni M, Chiumello D, Ranieri VM, Quintel M, et al. Lung recruitment in patients with the acute respiratory distress syndrome. N Engl J Med 2006;354:1775–86. https://doi.org/10.1056/NEJMoa052052.
[31] Bouhemad B, Richecoeur J, Lu Q, Malbouisson LM, Cluzel P, Rouby JJ. Effects of contrast material on computed tomographic measurements of lung volumes in patients with acute lung injury. Crit Care 2003;7:63–71. https://doi.org/10.1186/cc1852.
[32] Thille AW, Esteban A, Fernández-Segoviano P, Rodriguez J-M, Aramburu J-A, Peñuelas O, et al. Comparison of the Berlin definition for acute respiratory distress syndrome with autopsy. Am J Respir Crit Care Med 2013;187:761–7. https://doi.org/10.1164/rccm.201211-1981OC.